

# Optimization of interferometric array configurations by “sieving” $u - v$ points

Y. Su<sup>1</sup>, R. D. Nan<sup>1</sup>, B. Peng<sup>1</sup>, N. Roddis<sup>3</sup>, and J. F. Zhou<sup>2</sup>

<sup>1</sup> National Astronomical Observatories, Chinese Academy of Sciences, Chaoyang District, Datun Road 20A, Beijing, 100012, PR China

e-mail: [suyan@bao.ac.cn](mailto:suyan@bao.ac.cn); [nrd@bao.ac.cn](mailto:nrd@bao.ac.cn); [pb@bao.ac.cn](mailto:pb@bao.ac.cn)

<sup>2</sup> Center for Astrophysics, Tsinghua University, Beijing, 100084, PR China

e-mail: [zhoujf@tsinghua.edu.cn](mailto:zhoujf@tsinghua.edu.cn)

<sup>3</sup> Jodrell Bank Observatory, Dept. of Physics & Astronomy, the University of Manchester, Macclesfield, Cheshire SK11 9DL, UK

e-mail: [nr@jb.man.ac.uk](mailto:nr@jb.man.ac.uk)

Received 15 July 2003 / Accepted 10 October 2003

**Abstract.** A “sieving” algorithm, which gradually removes element candidates in a radio array to fit  $u - v$  distributions to a predefined shape, is introduced in this paper. The algorithm is applicable for optimizing the configuration of an interferometric array either in snapshot or Earth rotation synthesis observation mode. It has also been enhanced to do global array optimization when objects at different declinations are taken into account. To illustrate its efficiency, the sieving algorithm is employed to configure an optimum 30-element array from 2500 candidates within a circular or donut boundary. A preliminary C++ package implementing the algorithm has been developed for configuration designs and tests. The method is well adapted to general use due to flexibility and rapidity. For example, it has been tentatively applied to the optimization of the KARST array, a Chinese concept of the SKA.

**Key words.** instrumentation: interferometers – method: numerical

## 1. Introduction

Interferometers have existed for over 50 years in radio astronomy (Ryle 1952). In recent years, a similar technique has been applied to the optical waveband (Baldwin et al. 1996), and is likely to be extended into the X-ray waveband in the future (Cash 2000).

An interferometric array detects spatial frequencies of the sky brightness distribution, the visibilities, in the  $u - v$  plane by cross-correlating antennas pairs. A clean map of a radio object is then constructed by Fourier transformation and deconvolution, such as the CLEAN algorithm (Högbom 1974; Clark 1980) or the Maximum Entropy Method (Gull 1989). A uniform  $u - v$  distribution provides better sampling of the Fourier space of the image. In the absence of any prior information about the source structures to be observed, a uniform  $u - v$  distribution will offer a better signal-to-noise ratio with higher resolution. Sometimes, a Gaussian tapered  $u - v$  distribution is used to reduce the side-lobe level of the array beam, and to increase the detection sensitivity. In general, the

principle of designing arrays, therefore, is to obtain optimized  $u - v$  distributions that fulfil the requirements of the observations.

An optimum interferometric array configuration depends on source structures and positions, times of integration and scientific purpose (single field imaging, mosaicing etc.). Other constraints such as cost and geometrical locations should also be taken into account in a practical design of an array configuration. The large number of parameters and occasionally incompatible specifications make the optimization complex and difficult in a global solution.

To simplify array optimization, current interferometric array designs usually address a few specifications, which have been well covered by many authors. Cornwell (1986) proposed crystalline antenna arrays which were optimized by simulated annealing. Cornwell (1988) and Cornwell et al. (1993) studied interferometric imaging of very large objects and its implications for array design. An interferometric array with shapes based on slightly perturbed curves of constant width, in particular the Reuleaux triangle, was introduced by Keto (1997). Kogan (1997) put forward another approach from the point of view of minimizing side-lobe level, and further enhanced

---

Send offprint requests to: J. F. Zhou,  
e-mail: [zhoujf@tsinghua.edu.cn](mailto:zhoujf@tsinghua.edu.cn)

the algorithm with a donut constraint (Kogan 1998). The observing efficiency of a spiral zoom array, allowing for continuous scalability, was discussed by Conway (2000a,b). Woody (1999) discussed symmetric circular arrays with  $S$  identical sectors that achieved nearly complete coverage by Earth rotation synthesis over a limited hour angle range. Boone (2001) proposed an optimization algorithm which was based on the computation of pressure forces related to the discrepancies between the model and the actual distribution of Fourier samples.

The sieving method proposed here is based on the fact that the number of possible candidates is usually much larger than that required. Therefore, the corresponding  $u-v$  coverage of candidates is much denser than that of a desired array. This fact indicates that we should be able to gradually discard the candidates while keeping the  $u-v$  distribution shape which best approximates a desired sampling pattern. The candidates finally left are the optimized array configuration preferred. We, therefore, refer to this entire process as “sieving”.

The basic elements of the algorithm are described in the following sections, including definition of the weights of each  $u-v$  point and candidates for sieving, and global array optimizations. In Sect. 3, the algorithm is tested by optimizing array configurations for zenithal snapshot observations where elements are confined to a unit circle. In Sect. 4, primary results are presented as the method is applied to the KARST (Kilometer-square Area Radio Synthesis Telescope) array in Earth rotation synthesis observation mode. Brief concluding remarks are listed in the last section.

## 2. The sieving approach

As mentioned in the Introduction, the  $u-v$  distribution of candidates is usually much denser than that of the final array. We sieve initial  $u-v$  points from the entire candidate set to achieve either uniform or Gaussian shaped  $u-v$  coverage by iteratively selecting and removing  $u-v$  points. However, it should be noticed that each single  $u-v$  bit is not single antenna dependant since each antenna is related to a set of  $u-v$  points. We delete one candidate in each sieving step in the process according to numerical calculation of the weights of  $u-v$  points. The detailed process of sieving is given below.

### 2.1. Weights of $u-v$ points for sieving

In order to determine which  $u-v$  point should be removed in each iteration, quantitative estimation of the density of  $u-v$  points is made. At the first step, it is natural to simply start with a uniform weight. The uniform weight  $w_g$  of a  $u-v$  point is

$$w_g(i, j, t_k) = N_g^{-m}, \quad (1)$$

where  $m = 0, 1, 2, 3, \dots$  and  $N_g$  is the number of  $u-v$  points located in the same grid cell,  $i, j$  denoting two different candidates, and  $t_k$  is the observing epoch. We should remember that the weight defined above can't precisely distinguish very small differences of densities among the  $u-v$  points. For example,  $u-v$  points **A** and **C** in Fig. 1 are located in the same cell, and therefore have the same uniform weights according to Eq. (1).

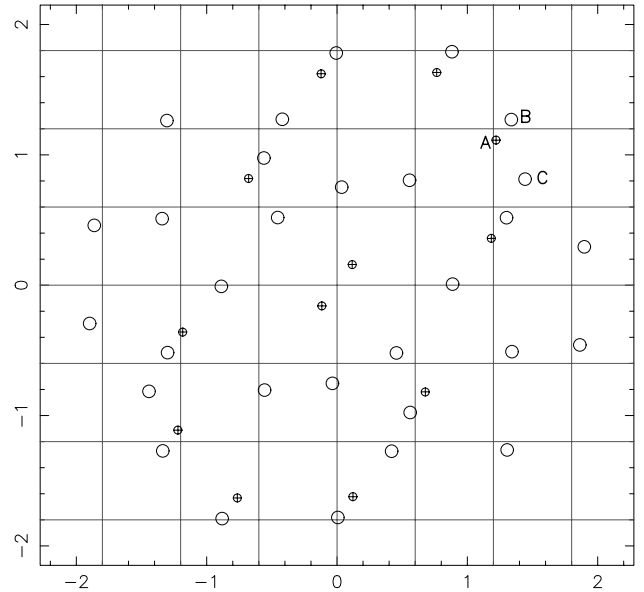


**Fig. 1.** The  $u-v$  coverage of snapshot observation of a 7-element array. The  $u-v$  points related to one element are represented by circles filled with a cross, and the others by open circles.

The  $u-v$  distributions around these two points, however, appear different. Point **C** seems to be in a sparser  $u-v$  area and should be kept, while point **A** in a denser  $u-v$  area, closely neighboring point **B**, so **A** should be removed for the uniform distribution although its weight is calculated as equal to **C**.

To properly define the weight of every  $u-v$  point as well as antenna for sieving, extra criteria need to be added. Here, we define a distance weight of a  $u-v$  point for evaluating the local  $u-v$  density in its vicinity. The weight is given by

$$w_d(i, j, t_k) = d_{\min}^n, \quad (2)$$

where  $d_{\min}$  is the distance between a  $u-v$  point and its nearest neighbor,  $n = 0, 1, 2, 3, \dots$ ,  $i, j$  and  $t_k$  are the same as defined in Eq. (1). For example, the distance weight  $d_{\min}$  of point **A** equals to the distance between **A** and **B**, since the closest point to **A** is **B** in Fig. 1.

The uniform and distance weights contain diverse information about the  $u-v$  distribution from different aspects. The uniform weight implies the density on large scales, while the distance weight indicates the local density around individual  $u-v$  point. To estimate each  $u-v$  point weight well for sieving, the uniform and distance weights should be combined in the evaluation. The hybrid weight can be described by

$$w(i, j, t_k) = d_{\min}^m N_g^{-m} \quad (m, n = 0, 1, 2, \dots) \quad (3)$$

where  $m, n$  and the size of the grid cell are modifiable parameters according to the requirements.

### 2.2. Append extra weight

The optimum array configuration depends strongly on source structure. Uniformly distributed  $u-v$  coverage has high angular resolution. This kind of  $u-v$  coverage is preferable for observing compact objects of simple structure. For extended sources,

the spatial spectra of source structures are mainly represented in small values of  $u$  and  $v$  which are always in the central region of the  $u - v$  plane. In order to obtain better images of the extended sources, the  $u - v$  coverage of an array should be denser in the central region and sparser in the outer part.

In order to meet this requirement, we can reduce the weights of  $u - v$  points in the outer region. Quantitatively, the defined weight of a  $u - v$  point  $w(i, j, t_k)$  can be tapered with a desirable function, such as a Gaussian. Therefore, the modified weight of a  $u - v$  point is

$$w'(i, j, t_k) = w(i, j, t_k) \left( (1 - w_{\min}) e^{-r^2/D^2} + w_{\min} \right), \quad (4)$$

where  $r$  is the distance between this  $u - v$  point and the origin of the  $u - v$  plane, while  $D$  and  $w_{\min}$  are free parameters used in adjusting the concentration of the  $u - v$  coverage.

### 2.3. Sieving algorithm

Considering the design of an  $M$ -element array from  $N$  candidates ( $M < N$ ), we can take the following steps:

1. According to the weight definition of each  $u - v$  point  $w(i, j, t_k)$  in Eq. (3) or  $w'(i, j, t_k)$  in Eq. (4), the weights  $W(i)$  ( $i = 1, 2, \dots, N$ ) of all the candidates are the sums of the relevant weights of the  $u - v$  points,

$$W(i) = 2 \sum_{j=1}^N \sum_{k=1}^K w(i, j, t_k) \quad (i \neq j), \quad (5)$$

where  $K$  is the number of data segments in Earth rotation synthesis observations.

2. For all candidates, try to find one which has the least weight  $W$ . Remove  $2(N - 1)$   $u - v$  points related to this element, and then  $N - 1$  candidates are left. Return to step 1, abandon other elements by repeating the same operation until only  $M$  elements remain.

In the above process, it is not proper to remove more than one candidate in each step, because the values and sequences of  $W(i)$  change as soon as one candidate is removed. The number and density of initial candidates will strongly influence the quality of the final optimum array configuration. The more and the denser the candidates, the better the final configuration and the greater the computing time. Approximately, the computing time is proportional to  $N^3$  in snapshot observation mode. A server equipped with an Intel Xeon 2.4 GHz CPU takes about 1 min to sieve out 30 elements from 250 candidates in snapshot observation mode. The computing time is about 20 hours for 2500 candidates.

### 2.4. Global array optimization

Since the array optimization also depends on the declinations of objects, an array may have various optimal configurations for sources at different declinations. Some arrays like the VLA (Very Large Array) and ALMA (Atacama Large Millimeter Array) have movable elements, and their array working modes are changeable for different observations. Other arrays such as

the EVN (European VLBI Network) and VLBA (Very Long Baseline Array) have fixed elements. To design such fixed element arrays, the compromise in a certain declination range is fundamental.

To do global array optimization, we still follow the sieving idea above. The weights however related to one candidate within a certain declination coverage are summed together as a global weight, which is applied to determine if this candidate should be removed or kept. Due to the differences of weightings at different declinations, normalization of the weights is required before summing. The actual global weight of each candidate is defined as follows,

$$W_N^d(i) = \frac{W^d(i) - \overline{W}^d}{\sigma^d} \quad (6)$$

$$W_G(i) = \sum_d W_N^d(i) \quad (7)$$

where  $W^d(i)$  is the weight (defined in Eq. (5)) of a candidate at declination  $d$ ,  $\overline{W}^d$  and  $\sigma^d$  are the average and variance of the weights respectively to the source at declination  $d$ ,  $W_N^d(i)$  is the normalized weight of a candidate at declination  $d$ ,  $W_G(i)$  is the global weight of a candidate.

During the global array optimization, we use the weight  $W_G(i)$  to indicate the importance of each candidate. In every sieving iteration, the candidate and its relevant  $u - v$  points with minimum  $W_G(i)$  are removed.

More selection criteria such as construction costs can also be merged into corresponding weights in practical implementation. For some unavoidable candidates, e.g. existing telescopes to be included in the configuration, their weights can be set large enough so that they would not be removed during the sieving algorithm.

We wrote a C++ package to realize the above algorithms with a number of weighting options. The basic data and function routines are encapsulated in a base class. Through overlying base weight functions by virtual functions, users can add extra weight functions in derived classes without modifying the original codes.

## 3. Applications in zenithal snapshot observation

To illustrate the usage and efficiency of the sieving algorithm, we begin by applying the algorithm to the optimization of an array configuration for a zenithal snapshot observation, assuming candidates are confined within a unit circle. The solution process is divided into the following steps. Firstly, randomly generate a large number of virtual candidates inside a unit circle; secondly, select a subset of the optimized array according to different predefined  $u - v$  distributions with the sieving algorithm, such as uniform (see Sect. 3.2) or Gaussian tapered (see Sect. 3.3)  $u - v$  distributions.

### 3.1. Setting the parameters

The determination of optimal parameters such as  $n$ ,  $m$  and the size of the grid cell in Eq. (3), is based on either theoretical deduction or experimental tests.

The preferable value of  $n$  is 2. Since  $d_{\min}$  is the distance between a  $u - v$  point and its nearest neighbor,  $d_{\min}^2$  can naturally be seen as a measure of the area that is occupied by a  $u - v$  point. Smaller  $d_{\min}^2$  means that a  $u - v$  point occupies less area and is probably in a denser  $u - v$  region. Such  $u - v$  points are more likely to be deleted in the sieving algorithm.

Other two important parameters,  $m$  and the size of the grid cell, are determined by a large number of tests. The sieving algorithm determines optimized array configurations from the different sets of random candidates with different values of  $m$  and the size of the grid cell. According to various aspects of the results, including the  $u - v$  coverage, the shape of the beam pattern and side-lobe level of the beam, we have verified different values of the parameters, and determined proper values to give the most satisfactory results.

It is found that  $n = 2$  and  $m = 2$  are preferable to optimize the array configuration either for uniform or Gaussian tapered  $u - v$  distribution. Furthermore, adaptive grid cell sizes at each iteration may be necessary, i.e., after taking out the  $u - v$  points related to a “bad” candidate, the remaining  $u - v$  points need to be re-gridded so that a cell contains an appropriate number of  $u - v$  points on average, e.g. 9 in our experiments.

### 3.2. Aim for uniform $u - v$ distribution

To find good array configurations which are optimized for a uniform  $u - v$  coverage, 2500 randomly distributed candidates in a unit circle are considered. The sieving algorithm based on Eq. (3) is used to choose a 30-element array. Figure 2 shows the configuration of the optimum array and its  $u - v$  distribution. It is clear that the  $u - v$  distribution shows general uniformness except for the slightly high density in the central region. This is reasonable as there is no solution to guarantee an exact uniform  $u - v$  distribution (Boone 2001). For different set of 2500 randomly generated candidates, the optimized array shows a tiny variation in configuration, but the final  $u - v$  distribution and the array synthesis beams appear almost the same to each other.

The most notable feature in the above experiments lies in the fact that the elements of the optimized array tend to lie close to the edge (see Fig. 2), which occurs for various sets of 2500 random candidates. Such array configurations are very similar when compared with the results by Cornwell (1986) and Keto (1997).

Since optimized elements tend to locate nearly on the circular boundary, we then confine a candidate set to an annulus. The candidates, therefore, distribute much more densely, and improved solutions are expected. Figure 3 shows the configuration of the selected array and its  $u - v$  distribution under the donut constraint, where the radius of the donut is  $0.9 < r < 1.0$ .

Figure 4 shows the beams of array configurations in Figs. 2 and 3. It can be seen that the beam pattern on the right is slightly rounder and the side lobe levels are lower.

### 3.3. Aim for Gaussian tapered $u - v$ distributions

As mentioned in Sect. 2.2, extra weights can be introduced to control the shape of the  $u - v$  distribution of an optimized array.

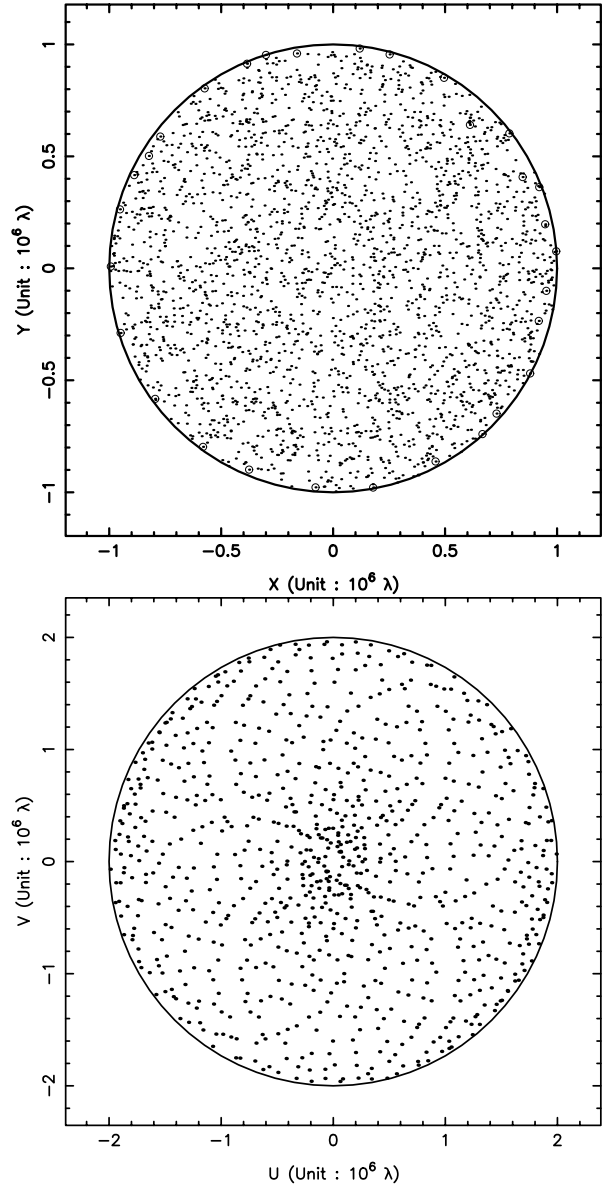


**Fig. 2.** Optimization example 1. The array is optimized for a zenithal snapshot observation. The  $u - v$  distribution obtained is uniform. Top: the original 2500 candidates (shown as points) are randomly distributed inside a unit circle. The selected 30 elements are indicated by small circles. Bottom: the snapshot  $u - v$  coverage of the selected elements.

The weights given by Eq. (4) are applied to an optimized array to achieve a Gaussian tapered  $u - v$  distribution. The optimized array configuration of 60 elements from 2500 candidates, and its  $u - v$  distribution are shown in Fig. 5, where the parameters  $w_{\min} = 0.00001$ ,  $D = 0.8 (10^6 \lambda)$ ,  $n = 2$  and  $m = 2$ . The array beam pattern is shown in Fig. 6. The FWHM of the beam, as expected, is wider than those in the examples 1 and 2 with the uniform  $u - v$  distribution. The side lobe levels of the beam, however, are much lower.

It is shown in Fig. 5 that some of the selected elements also lie very close to the circular edge, resembling those in the optimization for the uniform  $u - v$  distribution discussed above. The remaining selected elements, however, tend to spread over

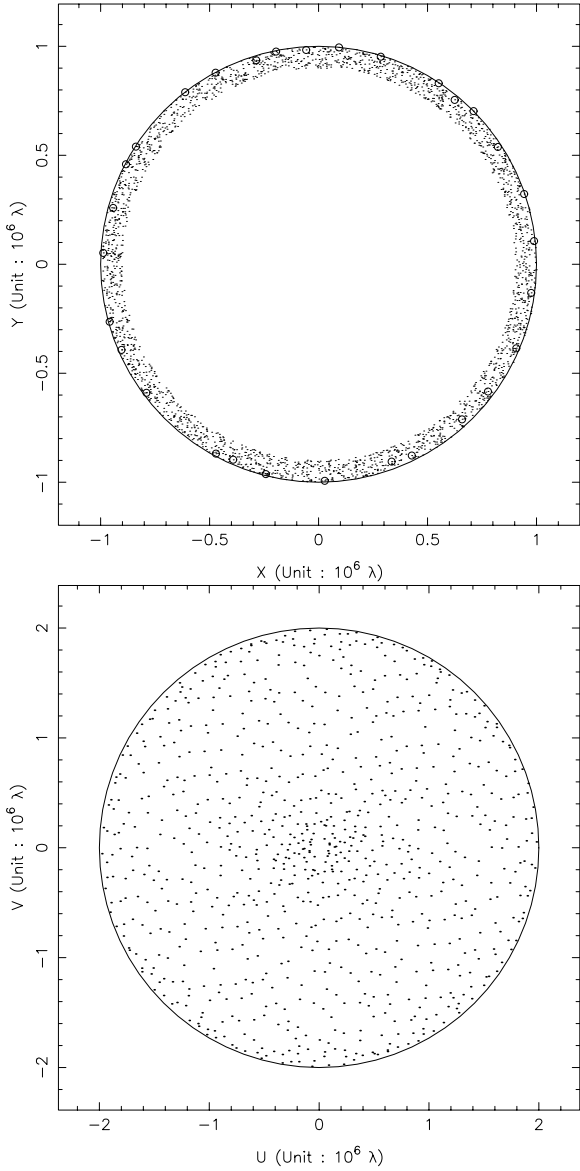


**Fig. 3.** Optimization example 2. The array is optimized for a zenithal snapshot observation. The  $u - v$  distribution obtained is uniform. Top: the original 2500 candidates (shown in points) are randomly distributed inside a donut, with radius between 0.9 and 1.0. Selected 30 elements are indicated by small circles. Bottom: the snapshot  $u - v$  coverage of 30 selected elements.

a large portion of the whole area. Such a configuration comes similar to that of Boone (2001), although we allocate more elements close to the edge.

#### 4. Applications in Earth rotation synthesis mode for Chinese SKA concept

The KARST, the Chinese contribution to the international SKA cooperation (Peng & Nan 1997), consists of about 30 FAST (Five-hundred-meter Aperture Spherical Telescope) type elements which will be sited in a karst topography. Several hundred karst depressions in the south of Guizhou province have been surveyed and studied (Nan et al. 1995). It is natural and necessary to select an optimized subset of elements

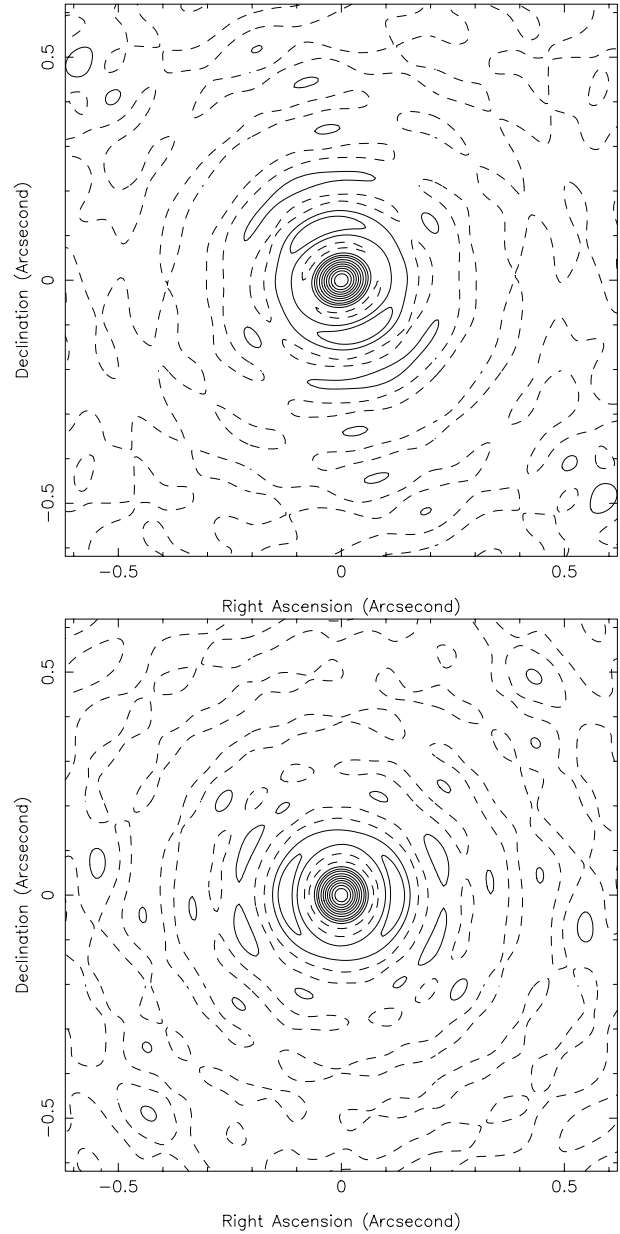


**Fig. 4.** The beams of optimized arrays in example 1 (Top) and example 2 (Bottom). The contour levels are  $-1.7, 6.7, 13, 20, 30, 40, 50, 60, 70, 80, 90\%$  of the peak.

from candidate depressions for the future antenna locations of the KARST. Since the length of the longest baseline in the east-west direction is about twice that in the north-south direction (see Fig. 7), Earth rotation synthesis is employed to achieve a better  $u - v$  distribution. The sieving algorithm is suitable for this kind of array optimization.

##### 4.1. Optimization for sources of fixed declinations

First, we optimize the KARST array for observing objects of fixed declination. During the experiments, two declinations of  $\delta = 60^\circ$  and  $30^\circ$  were considered. The observing wavelength was taken to be 18 cm. The number of karst depression candidates was set to 288, and that of the required elements was assumed to be 30. Each Earth rotation synthesis observation was

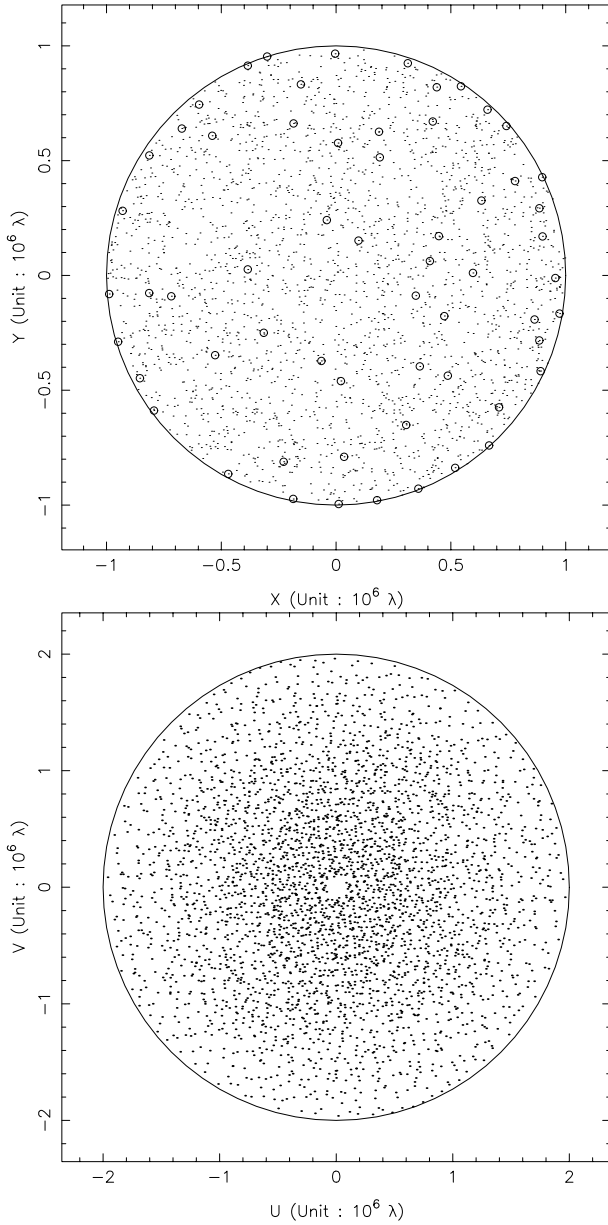


**Fig. 5.** Optimization example 3. The array is optimized for a zenithal snapshot observation. The  $u - v$  distribution obtained is Gaussian tapered with  $D = 0.8(10^6 \lambda)$  and  $w_{\min} = 0.00001$ . Top: the 2500 candidates are indicated by dots, and the selected 60 elements represented by small circles. Bottom: the snapshot  $u - v$  coverage of the selected elements.

composed of ten snapshot observations at 1.2 hour intervals. The optimized results for a uniform  $u - v$  distribution, including array configurations and their  $u - v$  distributions, are shown in Figs. 7 and 8.

The optimized arrays have different configurations at the two declinations, with 16 elements unshifted among 30. In the  $u - v$  plane, most  $u - v$  points are distributed uniformly, although the result is not as satisfactory as those of examples 1 and 2 in Sect. 3. The  $u - v$  distribution in the central region shows visible concentrations. Such a  $u - v$  coverage is due to the fact that the 288 depression candidates are already confined to a very limited region elongated in the east-west direction. It should be noted that there are more karst depressions being investigated

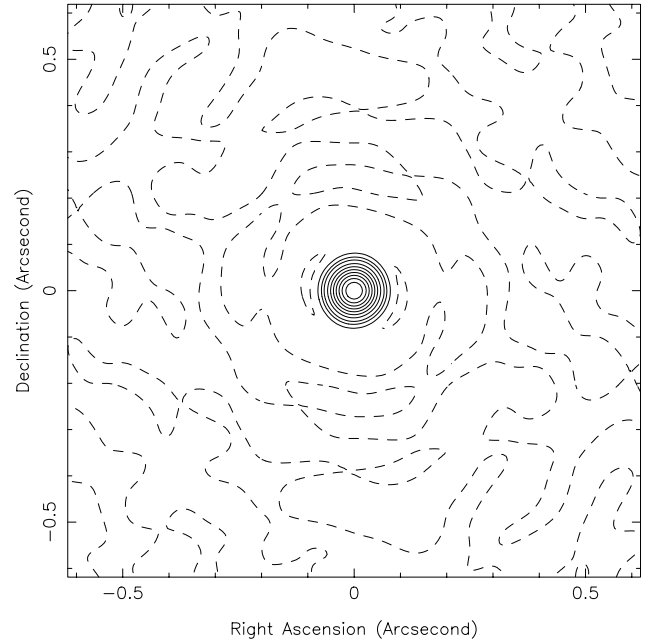


**Fig. 6.** The beam of the optimized array configuration in example 3. The contour levels are  $-0.8, 6.7, 13, 20, 30, 40, 50, 60, 70, 80, 90\%$  of the peak.

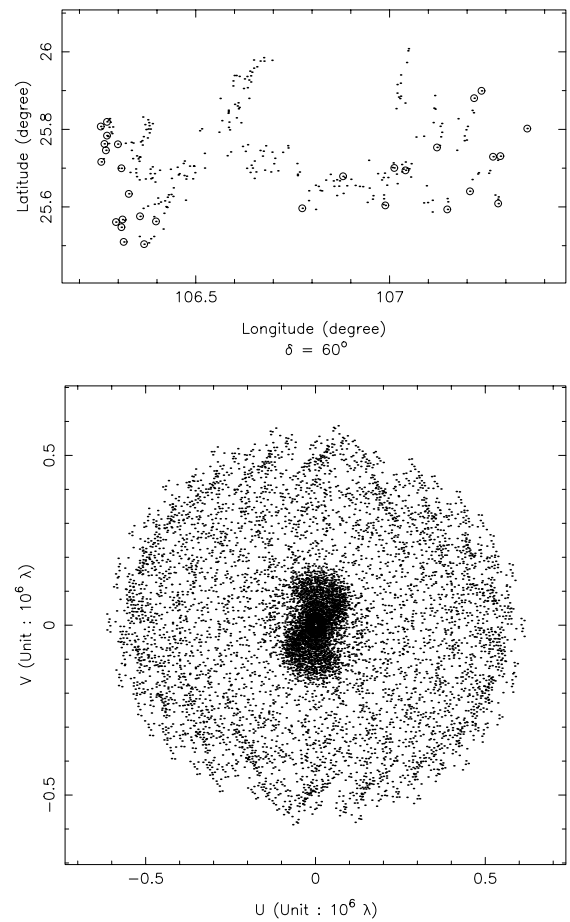


**Fig. 7.** Optimization of KARST in Earth rotation synthesis mode, aimed at a uniform  $u - v$  distribution. The declination of the source is  $60^\circ$ . The distribution of 288 candidates (points) in Pingtang county and 30 selected elements (circles) are shown on the top. The corresponding  $u - v$  coverage of the optimum array is shown at the bottom.

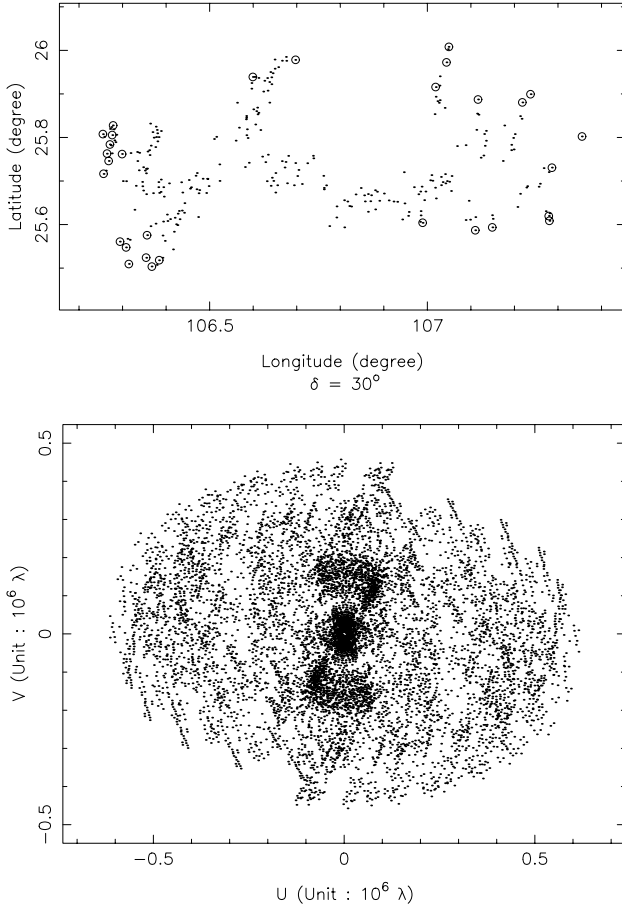


**Fig. 8.** Optimization of KARST in Earth rotation synthesis mode, aimed at a uniform  $u - v$  distribution. The source's declination is  $30^\circ$ . The distribution of 288 candidates (points) in Pingtang county and 30 selected elements (circles) are shown on the top. The corresponding  $u - v$  coverage of the optimum array is shown at the bottom.

in other neighboring counties for further consideration (Tian et al. 1995). As those candidates are included, the  $u - v$  distribution will certainly be improved.

To get a Gaussian tapered  $u - v$  distribution, we also carried out another optimization to select the KARST array, observing a source at a declination of  $60^\circ$ . The observing wavelength was also set to be 18 cm. The observation is composed of ten snapshot observations, with 1.2 hour intervals. The parameters were  $D = 0.2 (10^6 \lambda)$ ,  $n = 2$ ,  $m = 2$  and  $w_{\min} = 0.001$ . The optimized results are shown in Fig. 9.

#### 4.2. Global optimization of KARST array

An array will have different optimized configurations when observing sources at different declinations. To design a fixed array like KARST, therefore, the global array optimization algorithm described in Sect. 2.4 is preferable.

During global optimization, twelve declinations from  $90^\circ$  to  $-20^\circ$  at  $10^\circ$  intervals are considered, and the Earth rotation synthesis observation is composed of ten snapshot observations with 1.2 hour intervals. Other parameters are  $n = 2$  and  $m = 2$ . The optimum array aims for a uniform  $u - v$

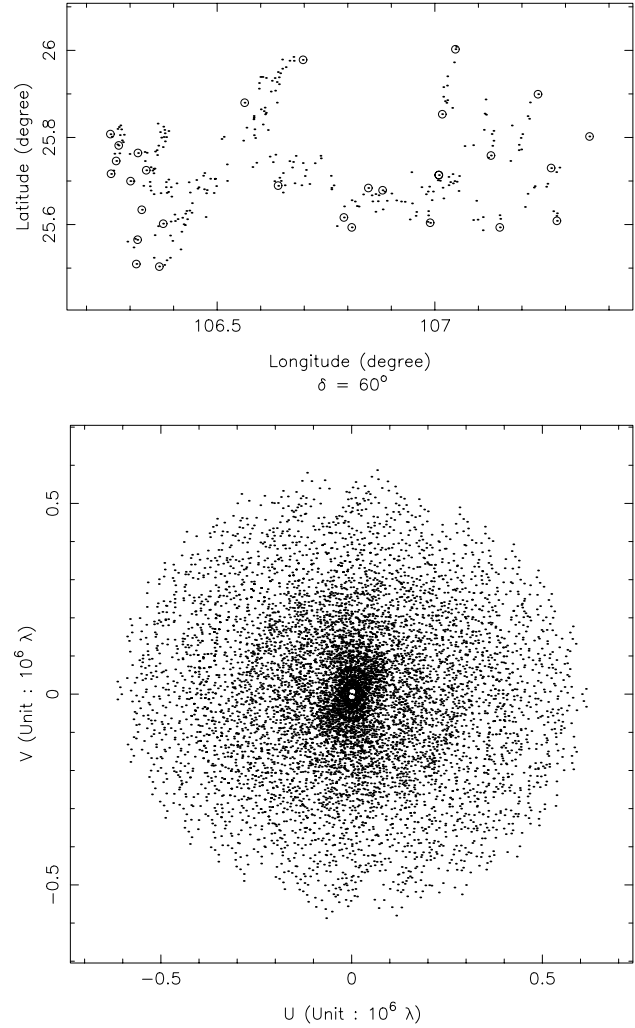


**Fig. 9.** Optimization of KARST in Earth rotation synthesis mode, aimed at a Gaussian tapered  $u - v$  distribution. The source's declination is  $60^\circ$ . The distribution of 288 candidates (points) in Pingtang county and 30 selected elements (circles) are shown on the top. The corresponding  $u - v$  coverage of the optimum array is shown at the bottom.

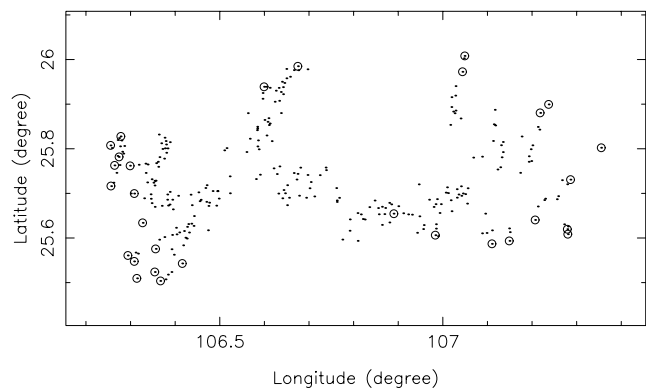


**Fig. 10.** The configuration of the KARST array which is derived by the global optimization algorithm.

distribution. Figures 10 and 11 show the array configuration and the corresponding  $u - v$  coverage at different declinations.

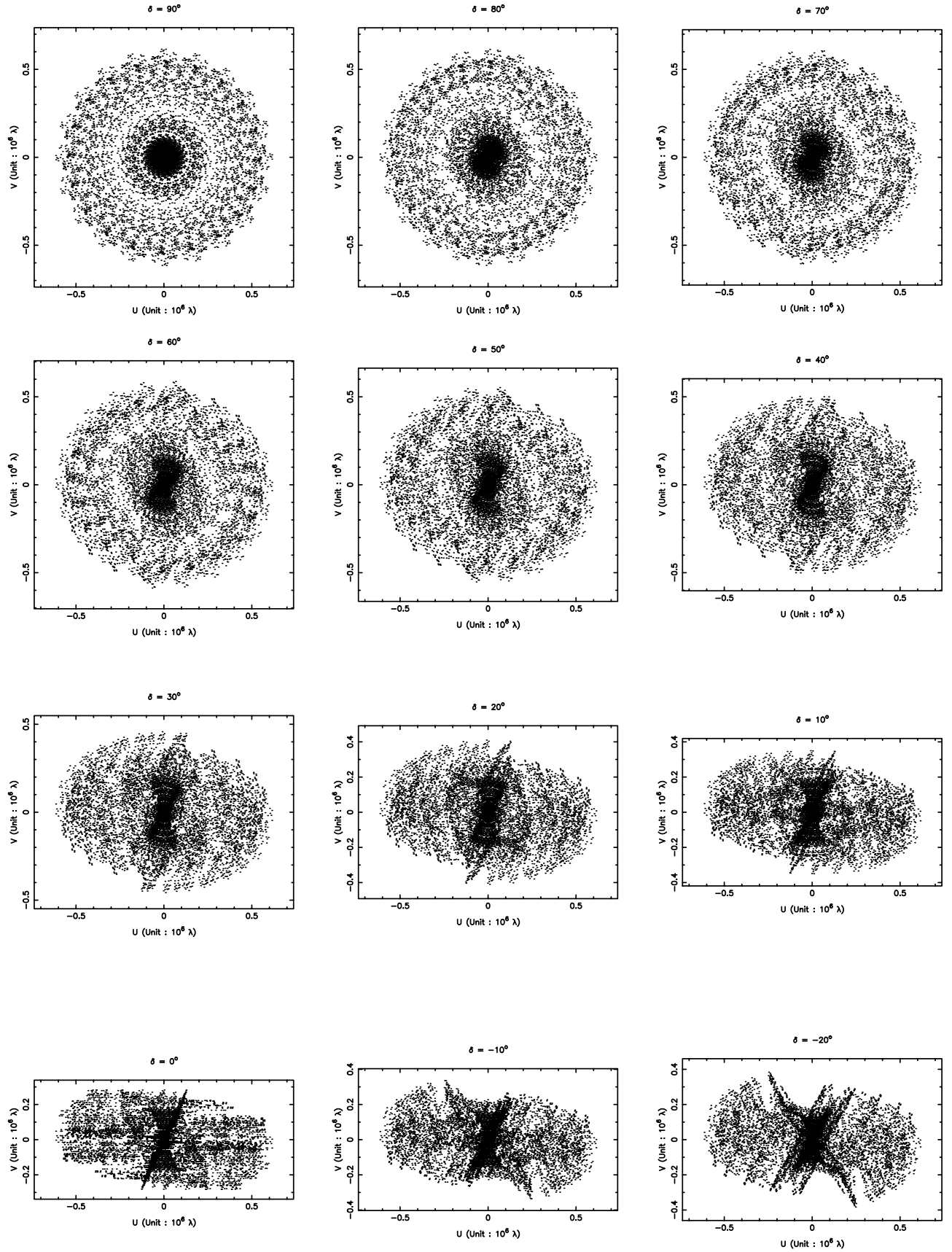


**Fig. 11.** The  $u-v$  distribution of the globally optimized KARST array at different declinations.

## 5. Conclusions

A new sieving algorithm is introduced to optimize interferometric array configurations. It is based on the fact that the  $u - v$  distribution of candidate elements is usually much denser than that of the selected array. Mathematical formulas and algorithms are developed to solve various array optimizations, including arrays for zenithal snapshot mode and Earth rotation synthesis mode, arrays aimed for uniform or Gaussian tapered  $u - v$  distributions, and arrays optimized for observing sources within a range of declinations.

The sieving algorithm offers some advantages for practical array designs. Firstly, the algorithm is able to globally search an optimized array configuration through all possible solutions, avoiding solutions in local minima. Secondly, it can handle interferometric arrays of different sizes, with the number of elements ranging from a few to several hundred. In addition, the computation time mainly depends upon the number of candidates, rather than the number of elements in the final optimized arrays. Finally, the algorithm is very flexible and expandable. Other factors related to array design can easily be introduced into the sieving algorithm, e.g. existing elements, infrastructure, project cost, etc.

A C++ package named *Sieve* has been developed to carry out the sieving procedure. Several examples as demonstration are presented to illustrate the algorithm's efficiency. It is found that the elements of an optimum array, which has a uniform  $u - v$  distribution, tend to appear very close to the boundary. The optimum array, with a Gaussian tapered  $u - v$  distribution, displays a new and interesting configuration which is different from those obtained by other optimizing algorithms. Finally, the sieving algorithm has been used to optimize the KARST array, a Chinese concept of SKA.

*Acknowledgements.* We thank an anonymous referee for constructive comments on this paper. We are grateful to Wim Brouw for carefully reading the manuscript and for helpful suggestions. We also thank Richard Strom for smoothing the paper. Peng acknowledges the NSF

of China through grant No. 10173015. Su, Nan and Peng acknowledge grant NKBRFSF 2003CB716703.

## References

- Baldwin, J. E., Beckett, M. G., Boysen, R. C., et al. 1996, A&A, 306, L13
- Boone, F. 2001, A&A, 377, 368
- Borck, D. 2000, ATA Memo, 15
- Borck, D. 2001, ATA Memo, 21
- Bunton, J. 1999, CSIRO Telecommunications and Industrial Physics, <http://www.atnf.cs-iro.au/projects/ska/techdocs/>
- Bunton, J. 2000, talk in SKA workshop on array configuration design, <http://www.jb.man.ac.uk/ska/workshop/Bunton5.pdf>
- Cash, W., Shipley, A., Osterman, S., & Joy, M. 2000, Nature, 407, 160
- Clark, B. G. 1980, A&A, 89, 377
- Conway, J. 2000a, in ALMA memo, 283
- Conway, J. 2000b, in ALMA memo, 292
- Cornwell, T. J. 1986, in ALMA memo, 38
- Cornwell, T. J. 1988, A&A, 202, 316
- Cornwell, T. J., Holdaway, M. A., & Uson, J. M. 1993, A&A, 271, 697
- Gull, S. F. 1989, in Maximum Entropy and Bayesian Methods, ed. J. Skilling (Dordrech: Kluwer), 53
- Hjellming, R. M. 1989, Synthesis imaging in radio astronomy, ed. R. A. Perley, F. R. Schwab, & A. H. Bridle, ASP Conf. Ser., 6, 477
- Högbom, J. 1974, A&AS, 15, 417
- Keto, E. 1997, ApJ, 475, 843
- Kogan, L. 1997, in MMA Memo, 171
- Kogan, L. 1998, in MMA Memo, 212
- Nan, R., Nie, Y., & Peng, B. 1996, Proc. of the 3rd Meeting of the Large Telescope Working Group and a Workshop on Spherical Radio Telescopes, ed. R. Strom, B. Peng, & R. Nan, 59
- Peng, B., & Nan, R. 1997, IAU Symp., 179, 93
- Ryle, M. 1952, Proc. of the Royal Society of London. Ser. A, Mathematical and Physical Sciences, 211, 351
- Tian, W., Qiu, Y., & Peng, B. 1996, Proc. of the 3rd Meeting of the Large Telescope, ed. R. Strom, B. Peng, & R. Nan, Working Group and a Workshop on Spherical Radio Telescopes, 188
- Woody, D. 1999, in ALMA memo, 270